Technical Paper

ISSN 1997-1400 Int. J. Pavement Res. Technol. 7(2):135-144

Reduction of Pavement High Temperature with the Use of Thermal Insulation Layer and High Reflectivity Surface

Rajib B. Mallick[1+], Bao-Liang Chen[1], A. Veeraragavan[2], G. L. Sivakumar Babu[3], and Sankha Bhowmick[4]

Abstract: This paper presents a study that was conducted to evaluate the concept of using an insulation layer along with a relatively high reflectivity surface for insulating pavements from extremes of temperature. Both finite element modeling (FEM) and experiments were carried out. FEM models were used to evaluate the effectiveness of higher reflectivity and lower conductivity on the temperature of the HMA pavement. Combinations of geosynthetic (as insulation) with and without chip seals (with partially exposed light colored aggregates as high reflectivity surface) were studied with experiments that were conducted with actual solar radiation. Temperature data were collected at the surface and at various depths. The temperature at different depths of the samples with the geosynthetic reinforced chip seal (GRCS) were found to be lower than that of the conventional hot mix asphalt (HMA) sample. The reduction in temperature is greater at higher solar radiations and warmer temperatures. It can be concluded that a GRCS can be used effectively to reduce the temperature of asphalt pavements and help in reducing their rutting potential.

DOI:10.6135/ijprt.org.tw/2014.7(2).135
***Key words**: Chip seal; Geosynthetic; Insulation; Reflectivity; Rutting.*

Introduction

High temperature related failures continue to be a major challenge for asphalt pavements. An increase in temperature of asphalt pavements leads to a lowering of the modulus of hot mix asphalt (HMA) and hence an increase in the potential of permanent deformation or rutting [1-7]. Fig. 1 shows examples of change in dynamic modulus of HMA with a change in temperature. Although in this paper the discussions are based on the increase in rutting potential, a rise in temperature will also cause faster aging [8-10] of the asphalt, and cause increase in the potential of fatigue cracking due to increased stiffness caused by faster aging.

Several approaches have been proposed to prevent high temperature related pavement deformation. The use of modifiers and appropriately performance graded (PG) asphalts are therefore utilized for making HMA resistant to rutting, specifically when high temperatures and/or heavy and slow moving traffic are expected [11]. Studies have been conducted to use flowing water through embedded pipes to cool pavements as well to use retained water in layers underneath the surface [12, 13]. Research is also underway to develop the appropriate conductive spreader material to reduce the number of pipes underneath pavements [14].

[1] Civil and Environmental Engineering Department, Worcester Polytechnic Institute (WPI), 100 Institute Road, Worcester, MA 01609, USA.
[2] Civil Engineering Department, Indian Institute of Technology (IIT) Madras, Chennai 600 036, Tamil Nadu, India.
[3] Department of Civil Engineering, Indian Institute of Science (IISc) Bangalore, Bangalore 560012, Karnataka, India.
[4] Department of Mechanical Engineering, University of Massachusetts, Dartmouth, 285 Old Westport Road, North Dartmouth, MA 02747-2300, USA.
[+] Corresponding Author: E-mail rajib@WPI.EDU
Note: Submitted March 23, 2013; Revised November 18, 2013; Accepted November 20, 2013.

An alternative method of reducing the rutting potential is proposed here. A thin insulating layer could be placed near the top of the pavement to prevent the temperature from increasing to a level where rutting is expected (in the range of > 35-40°C). By placing a thin insulating layer close to the surface, one can prevent the majority of the pavement from heating up. To prevent the accumulation of heat in the top layer, a high reflectivity surface (high reflectivity means in the range of 0.2-0.5; please see Table 1 for some common values) could be used. If the insulation and the high reflectivity surface can be used together effectively, then the temperature at the surface as well as the lower layers of the asphalt pavement can be reduced, and this can lead to a reduction of rutting potential, and slow down the aging of HMA, thus reducing the potential of fatigue cracking also. Note that the high reflectivity surface will lower the surface temperature, while the insulation close to the surface will insulate the lower layers. This can extend the lives of pavements, prolong the maintenance cycles, reduce the

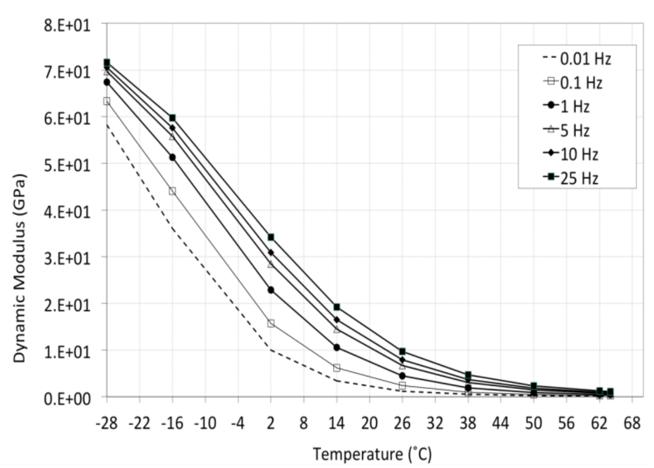

Fig. 1. Plot of a Typical Dynamic Modulus Versus Temperature Data for a HMA Mix.

Table 1. Reflectivity of Some Materials as Reported in Reference [15]

Material	Reflectivity
Asphalt	0.09
Aged Asphalt	0.14
Concrete	0.29
Grass (green lawn)	0.19

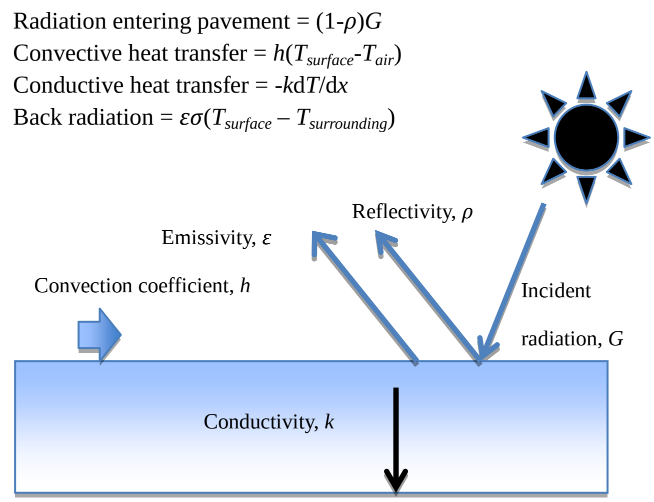

Fig. 2. Thermal Properties and Mechanisms Associated with Heating of Pavement Due to Solar Radiation.

use of materials, energy and money, help avoid construction related delays for the traveling, public, reduce near surface air temperature, reduce emissions resulting from construction and maintenance activities, and hence would be a true step towards building sustainable pavements.

The objective of this study is to present modeling/simulation and experimental study results to illustrate the use and possible efficacy of insulation of asphalt pavement. The scope of work reported in this study includes both modeling/simulation and experimental work. Finite Element modeling (FEM) of different pavements and simulation (with realistic sinusoidal solar radiation) were carried out to determine the effect of providing insulation with and without high reflectivity surfaces on pavement and near surface air temperatures. Next, experiments were conducted to validate the findings of the models. In the experiments, a geotextile layer (made of polypropylene) and a chip seal with a locally available light colored aggregates were utilized as insulation and high reflectivity layers, respectively.

Background

Solar radiation absorbed by an asphalt pavement raises its temperature. There are four predominant mechanisms in the transfer of heat to a pavement, as shown in Fig. 2 [16]: solar radiation in and emitted radiation out of the pavement, conductive transfer of heat through the pavement, and convective transfer of heat above the pavement through wind. Due to the very nature of the material, an asphalt pavement has a high absorptivity (0.85-0.93 [17], and hence a low reflectivity) to solar radiation. At the same time its low conductivity (0.76-1.4 W/m.K, [14]) prevents the absorbed energy from being transported elsewhere. This, coupled with relatively high thermal capacity (921-1,674 J/kg.K [18]) of the asphalt mixture, causes storage and concomitant rise in pavement temperature.

The different parameters mentioned in Fig. 2 are explained as follows. The total incident radiation is composed of three components, absorptivity (α), reflectivity (ρ), and transmissivity (τ); and the sum of the three components is equal to one.

$$\alpha + \rho + \tau = 1 \tag{1}$$

Absorptivity is the fraction of the total incident radiation that is absorbed by the surface, reflectivity is the fraction of the total incident radiation reflected by the surface, and the transmissivity is the fraction of the total incident that is transmitted through the body.

$$\alpha = \frac{absorbed\ radiation}{incident\ radiation}$$

$$\rho = \frac{reflected\ radiation}{incident\ radiation}$$

$$\tau = \frac{transmitted\ radiation}{incident\ radiation}$$

Transmissivity is equal to zero for most solid surface since the bodies are usually opaque to the incident radiation, and the total incident radiation therefore becomes the sum of the absorptivity and reflectivity.

$$\alpha + \rho = 1 \tag{2}$$

The incident radiation can be measured by pointing a hemispherical surface of pyranometer vertically toward the sky, and the back-radiation from the HMA surface can be measured by pointing the hemispherical surface of pyranometer vertically toward the HMA surface [19]. Example calculations for a 5 year-old HMA pavement are shown in Table 2.

The emissivity (ε) of HMA can be determined by using Kirchhoff's law of thermal radiation where the emissivity is equal to absorptivity for an object in thermal equilibrium. In this case, therefore, the emissivity of the HMA was 0.91.

From Fig. 2, it is clear that a way of preventing pavement temperature increase is either by lowering the conductive heat transmission (kdT/dx component) or minimizing the absorbed solar radiation (increasing alpha). The proposed hypothesis for this work is that if a relatively low conductivity material could be used near

Table 2. Field Measurement of Incident Radiation [17].

Incident Radiation (A)(W/m^2)	Back-radiation (B) (W/m^2)	Calculated Absorptivity (C) (%) (100%B/A)	Calculated Reflectivity (D) (%) (1- C)
1050	95	91	9

the top of the pavement, then it would act as a thermal insulating layer (and reduce the conducted heat). For such insulation, a layer of material with relatively low thermal conductivity could be used near the surface of the pavement. An example of such material is a typical geotextile layer (2 mm thick), made up of polypropylene, which has a thermal conductivity of about one tenth of that of HMA (k~0.1 W/m.K), saturated with asphalt, which also has a low thermal conductivity of 0.1 W/m.K. The other approach in which the temperature of a pavement could be reduced, is by reflecting a greater part of the incoming solar radiation, through the use of a layer with a relatively higher reflectivity (as compared to HMA, which has a reflectivity of approximately 0.05-0.09). Such a reflective layer could be prepared with a chip seal (maximum size of aggregate is 6 mm). These two approaches were investigated in this paper. First, the concept was examined and validated by modeling and simulation, and next, experiments were carried out to evaluate the effectiveness of the concepts.

Modeling and Simulation

A HMA sample, and the temperature change within the sample, when subjected to a constant radiation (and absence of radiation) were modeled with finite element (FE) method. The details of modeling are as follows. One rectangular layer is created for the HMA sub-domain with the pre-determined thermal properties, thermal conductivity k = 1.2 W/m.K, heat capacity C = 1200 J/kg.K, and density ρ = 2350 kg/m^3 [18]. The HMA layer contains 544 triangular mesh elements and 1,147 degree of freedom.

Only topside of the HMA layer is exposed to the radiation of 1,000 W/m^2 with wind-speed of (1) 0 m/s and (2) 2.2 m/s (forced convective heat transfer coefficient is assumed), and the external temperature and emissivity of HMA are assumed as 25℃ and 0.9 respectively [20]. The external temperature was assumed arbitrarily to observe the effect of the radiation in terms of change in temperature. The other 3 sides of the HMA layer are assumed as thermally insulated boundary condition. The radiation profile is assumed as 8-hours no-radiation, 8-hours radiation, and 8-hours no-radiation for one-day cycle for the duration of 7 days. The transient condition is used for the model with time of 604,800 seconds (24 x 7 = 168 hours) and time step of 3600 seconds. The relatively high time step was selected to cover the fairly long simulation time of 168 hours. Schematics of the models are shown in Fig. 3.

The governing equations are as follows [12]:

Subdomain condition for asphalt pavement (conduction)

$$\rho_p C_p \frac{\partial T}{\partial t} + \nabla.\left(-k_p \Delta T\right) = Q + q_s T \quad (3)$$

Subdomain condition for air layer:

$$\rho_a C_a \frac{\partial T}{\partial t} + \nabla.\left(-k_a \Delta T\right) = Q + q_s T - \rho_a.C_a.u.\nabla T \quad (4)$$

Boundary condition (convection)

$$(-k_p \nabla T) = q_o + h\left(T_{inf} - T\right) + \epsilon\sigma\left(T_{amb}^4 - T^4\right) \quad (5)$$

$$h = \frac{k_a}{L}\frac{0.928 P_r^{0.33} R_e^{0.5}}{\left(1+\left(\frac{0.0207}{P_r}\right)^{0.67}\right)^{0.25}}$$

$$P_r = 2.8649 - 1.3494 logT + 0.1949 (logT)^2 \quad (6)$$

where,

ρ_p, ρ_a = density of pavement and air, respectively
C_p, C_a = specific heat of pavement and air, respectively
T = temperature
t = time
∇ = gradient
k_p, k_a = thermal conductivity of pavement and air, respectively
Q = heat source
q_s = absorption coefficient
q_o = heat flux
h = heat transfer coefficient
T_{inf} = external temperature
ϵ = emissivity of pavement
σ = Stefan-Boltzmann constant
T_{amb} = Ambient temperature
P_r = Prandtl number
R_e = Reynolds number

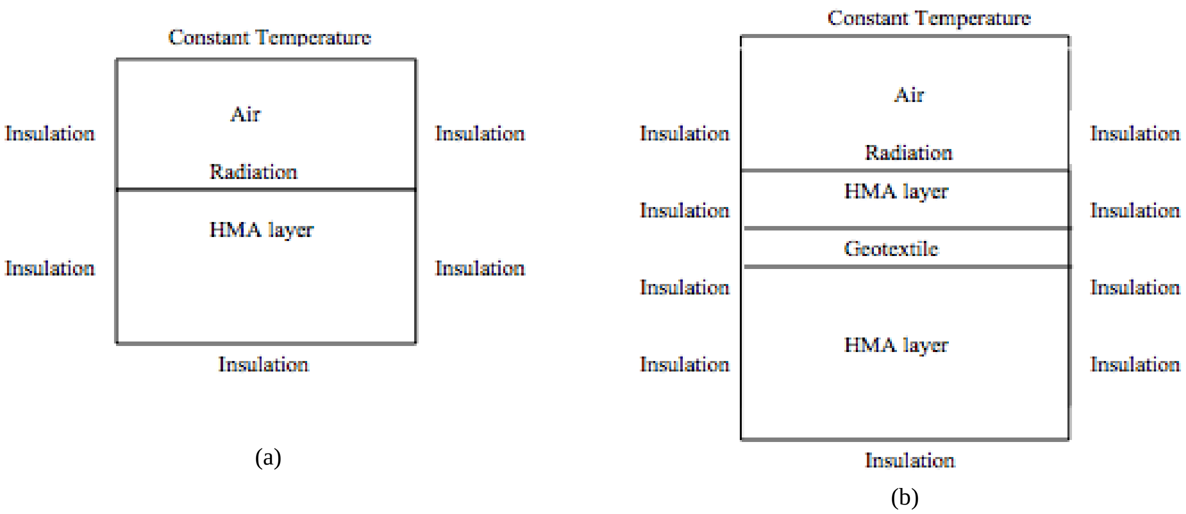

Fig. 3. Schematic of the Finite Element Models and Boundary Conditions; (a) HMA Only; (b) HMA with Geotextile.

Table 3. Thermal Properties of HMA and Geotextile (Plypropylene).

	Thermal Conductivity *k*, W/m.K	Heat Capacity *C*, J/kg.K	Density *ρ*, kg/m^3
HMA	1.2	1,200	2,350
Insulation	0.17*	904	1964

Note: * 0.17 W/m.K was used as it is the thermal conductivity of a common geosynthetic material, polypropylene [21].

Seven consecutive cycles of solar radiation and no-radiation were used. Each solar radiation period is 8 hours, with a constant radiation of 1,000 W/m^2; and each no-radiation period is 16 hours (total 7 times 24 hours of simulation). The 7 day simulation were carried out since the high temperature for design of asphalt pavement mixes is determined from the average of maximum HMA pavement temperature over a 7 day period through summer, which is obtained from weather stations data.

COMSOL (20, Heat Transfer and general modules) were utilized for modeling. COMSOL is a multiphysics finite element software that allows the modeling and simulation of a variety of mechanisms/processes (structural/heat transfer/chemical, for example) and accommodating the coupling effects of the different processes.

HMA + Insulation Model

Three rectangular layers are created for the HMA with insulation sub-domains with the thermal properties shown in Table 3. The insulation layer is inserted between two HMA layers. The entire geometry contains 620 triangular mesh elements and 1,307 degree of freedom.

The boundaries between HMA and polypropylene layers are assumed with interior boundary condition. The initial temperature of the HMA and polypropylene layers are assumed as 25℃ and the transient condition is used for the model with time of 60,4800 seconds (168 hours) with time step of 3600 seconds.

Results

The results of simulation are shown schematically in Fig. 4**.** It can be observed that, as expected, the temperature at a depth of 25 mm, which is below the insulation layer, is reduced as a result of the insulation (maximum temperature reduced by 9^{o}C, compared to HMA only); however, because of the blocking of heat conduction through the insulation layer, there is an increase in the surface temperature (an increase of 5^{o}C compared to HMA only). This increased surface temperature can lead to deformation of the surface layer, and will also lead to a higher near-surface air temperature, which is undesirable.

To avoid the higher surface temperature and still obtain the benefits of lower temperatures at points below the insulation, the concept of using a surface layer of relatively higher reflectivity is next applied [22-24]. A relatively higher reflectivity could be obtained for chip seals with partially exposed aggregates of light color.

To test this hypothesis, further simulations were carried out using

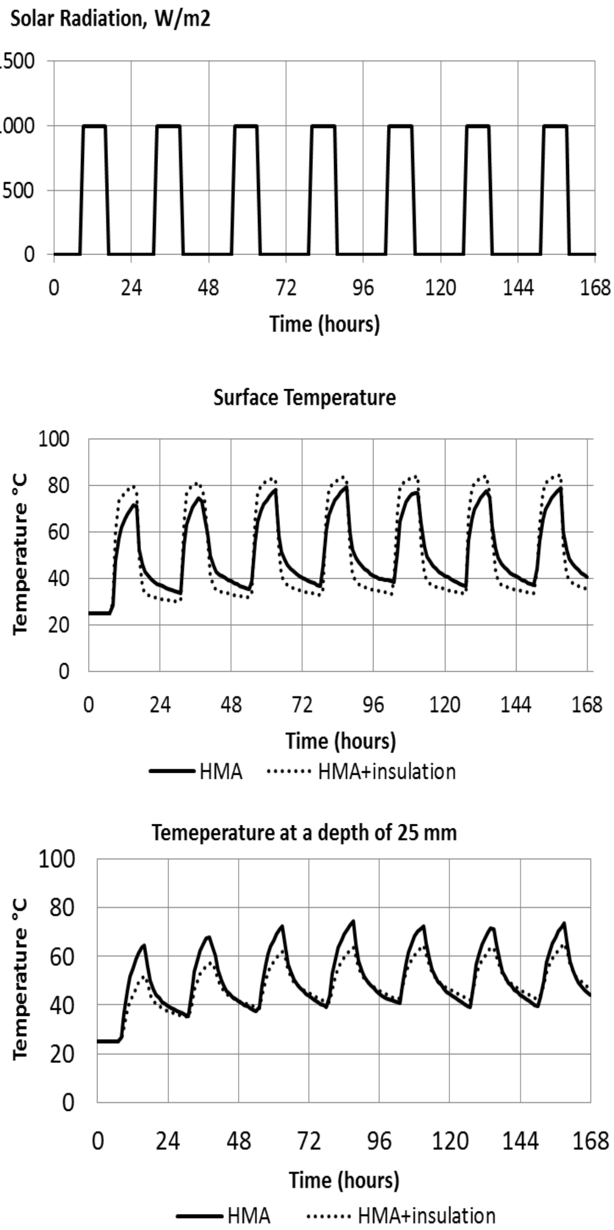

Fig. 4. Results of FEM Simulation.

a conventional HMA, and two with reflectivity of 0.25 and 0.5, respectively, with and without insulation. To investigate the effect in a very high solar radiation region (maximum radiation = 1,000 W/m^2), the solar radiation of Chennai (13.08N, 80.27E), India (for seven days following the maximum solar radiation first observed in a year, 2002, data obtained from National Renewable Energy Laboratory, NREL [25]) is shown in Fig. 5. Temperatures inside the pavement and above the pavement (air temperatures) upto a height of 100 mm were calculated and are shown in Fig. 6. The results show that the presence of a higher reflectivity surface and the geosynthetic layers contribute to significant lowering of surface and in-depth temperature as well as air temperature above the pavement. The decrease in temperature, for example, at the surface ranges from about 5℃ -15℃.

The NCHRP 1-37A Mechanistic Empirical Pavement Design Software (MEPDS [18]) was used for predicting the rutting damage

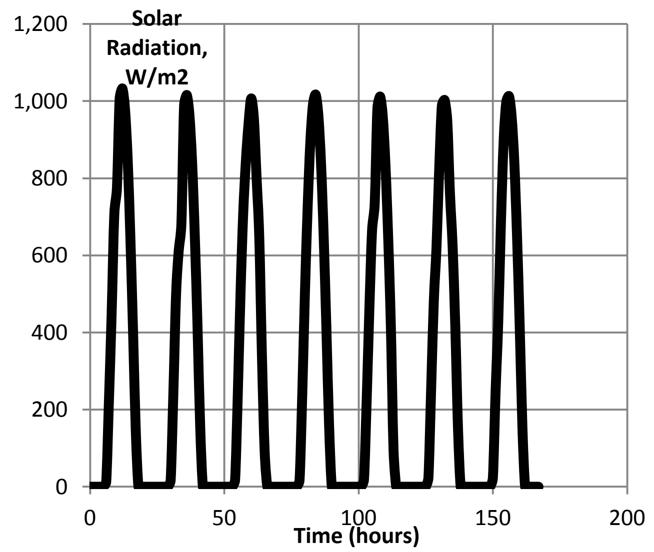

Fig. 5. Solar Radiation, Chennai, India.

over different years, considering the usual pavement temperature, and then a range of temperatures that are lower than the usual temperature. To do this, the climate database in the MEPDS was utilized. For this study, four US cities (FHWA, 2009 [26]*; note that even though FEM was carried out with radiation data of Chennai, India, the MEPDS simulations were carried out with these cities, since the climate data files in MEPDS are available only for US cities*) were selected to consider a range of maximum pavement temperatures, from 70 to 52°C. These are, in decreasing temperatures, Houston, TX, Raleigh-Durham, NC, Chicago, IL and Portland, ME. A pavement located in Houston was simulated, using the climatic information for the above four cities, to determine the rutting damage over the years, and the years to failure (for rutting due to the asphalt mix layer only), for the range of temperatures (70 to 52°C). The traffic and structure for the analyzed pavement in Table 4.

The pertinent results of simulations with the MEPDS are shown in Fig. 7. As expected, for the sample pavement and traffic, the life (rutting failure due to asphalt mix layer only) increases as the maximum pavement temperature decreases. For a change of maximum pavement temperature from 70°C to 52°C, the life increases from 8 to 20 years.

In the high temperature zone, each Celsius drop in temperature adds approximately one year to the service life of the pavement. Furthermore, the lowering of temperature decreases the aging potential significantly, and hence extends the fatigue cracking life of the pavement. Finally, the lowering of the near surface air temperature leads to significant environmental benefits such as in terms of reduction of near surface ozone concentration [27].

Experimental Work

To evaluate the concepts described and modeled earlier, experiments were carried out with HMA samples, which were subjected to solar radiation; in the first set of testing, the solar radiation was simulated with halogen lamp, and in the subsequent tests actual solar radiation was utilized. For insulation, a polypropylene geotextile layer was utilized, whereas for a surface with relatively high reflectivity, a geosynthetic reinforced chip seal (GRCS) was used [28]. For the chip seal, a locally available river gravel aggregates, conforming to

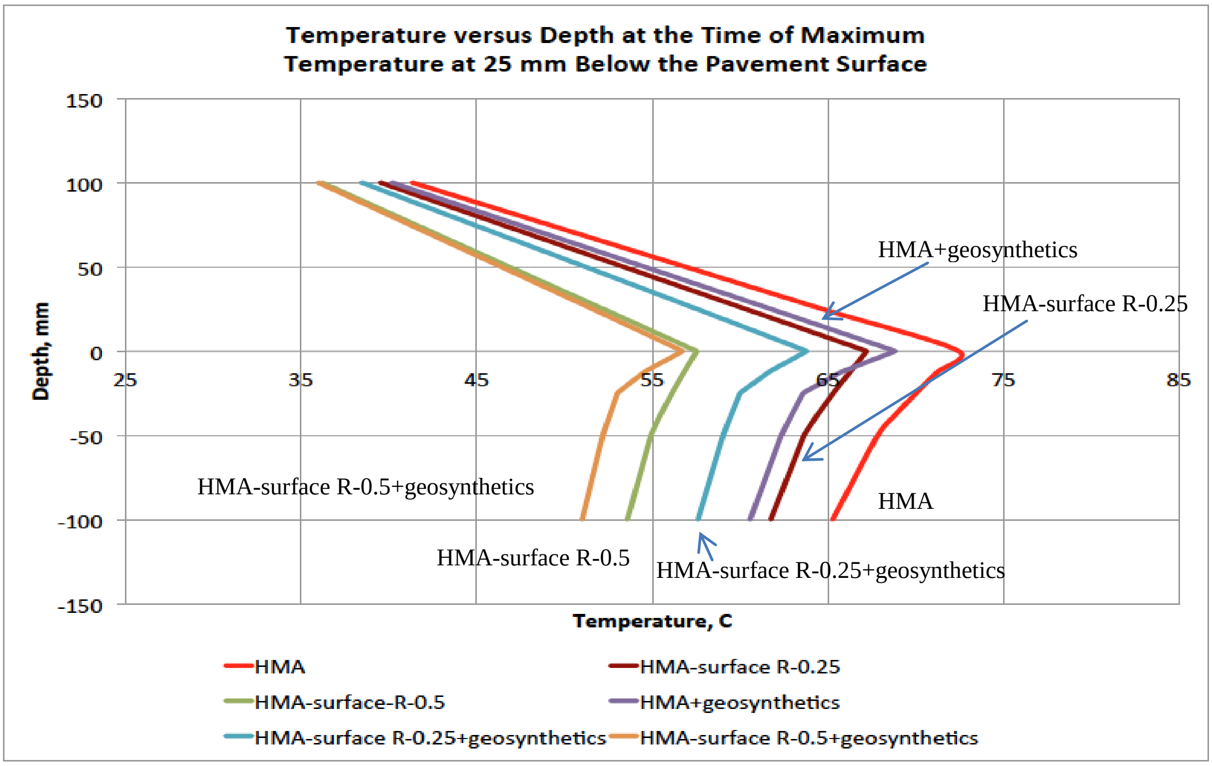

Fig. 6. Results of Simulation.

Table 4. Traffic and Pavement Data.

Parameter	Value
Traffic	
Initial Two-way AADTT	25,000
Number of Lanes in Design Direction	2
Percent of Trucks in Design Direction	50
Percent of Trucks in Design Lane	50
Operational Speed (mph)	60
Pavement	
HMA Layer: 4 inch; Binder	PG 70-28
Crushed Aggregate Base Course	12 inch
Subgrade Soil	A-2-4

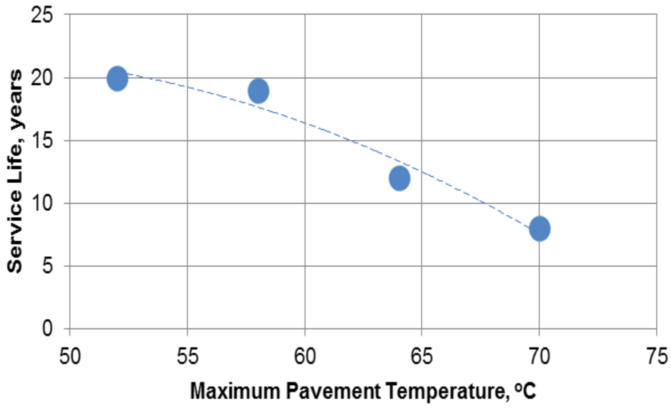

Fig. 7. Service Life Versus Maximum Pavement Temperature.

the gradation of chip seal and with reflectivity of 0.24 was utilized.

In the first set of experiments, tests were carried out with a conventional HMA sample, and the same sample with a geosynthetic reinforced chip seal. The steps in the preparation of the GRCS layer are as follows. First the surface of the sample was cleaned. Next a collar was placed around the sample to prevent draining of asphalt. A tack coat of PG 64-28 asphalt was then applied evenly across the top at a rate of 1.36 liters per square meter. The geotextile fabric was then placed as a disc on the sample, and compacted with a hand roller. Next a MS-2 emulsion was applied on top of the geotextile at a rate of 1.36 liter per square meter. After waiting for the emulsion to break, 9.5 mm nominal maximum aggregate size (NMAS) aggregates were then spread on the emulsion at a rate of 10.85 kg/m^2 and compacted to produce 70% embedment.

Tests were carried out for both windless and wind (2.2 m/s, 5 miles per hour) conditions. The sample was instrumented with thermocouples at different layers and temperatures were obtained during the entire length of the study.

The testing consisted of subjecting the sample to a radiation of 1,000 W/m^2 and 0 W/m^2, alternatively, using a halogen lamp, for 8/16 hours every day, for a total time period of 7 days. In the case in which wind was used, a table fan was utilized to obtain a wind speed of 2.2 m/s (5 mph). The radiation and the wind speed were checked with a pyranometer and an anemometer, respectively. Temperatures were measured at the surface, 25 mm below the surface, at the bottom and 25 mm above the bottom, and of the air, using *K* type thermocouples. The sample with geosynthetic

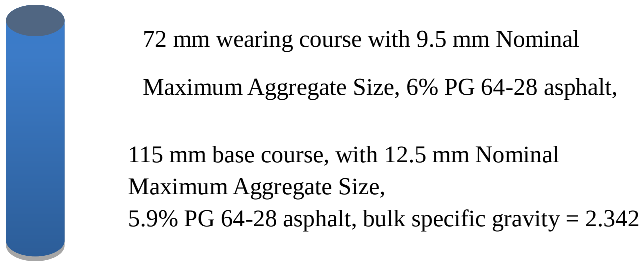

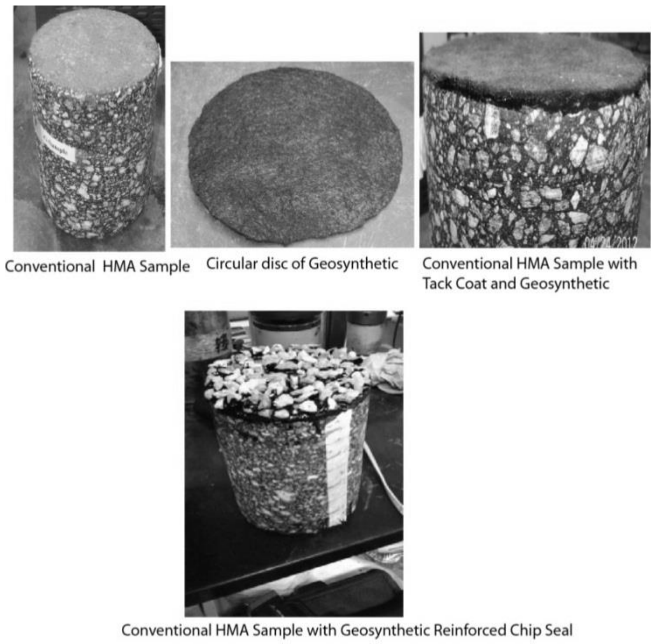

Fig. 8. Conventional HMA Sample and Sample with Geosynthetic Reinforced Chip Seal.

reinforced chip seal is shown in Fig. 8.

Results

The results of the experiments are summarized in Fig. 9. It can be seen that the maximum temperature at a depth of 25 mm is reduced by about 6-10°C, and the temperatures below 25 mm are also lower in the case of the GRCS sample. It shows the maximum temperature within the asphalt pavement is concentrated to a narrower zone by the presence of the geosynthetic reinforced chip seal layer. The significance is that less of the HMA pavement will now be subjected to a higher temperature and hence less of HMA will be subjected to the risk of rutting and aging.

In the next step, tests were carried out with laboratory prepared samples - a control sample and a sample with GRCS, using actual solar radiation. Both samples were tested at the same time, and solar radiation data and wind speed were continuously collected. Gradation of the mix is shown in Fig. 10; a PG 64-28 asphalt binder was used at 6% asphalt content, and the voids in total mix (VTM) of the control and the GRCS samples were found to be 5.0 and 4.4, respectively. Note that the experiments were conducted by the first author and his students at WPI, which is located in Massachusetts, USA. Therefore, a gradation that is used by Massachusetts Highway Department was utilized for the preparation of the sample. The

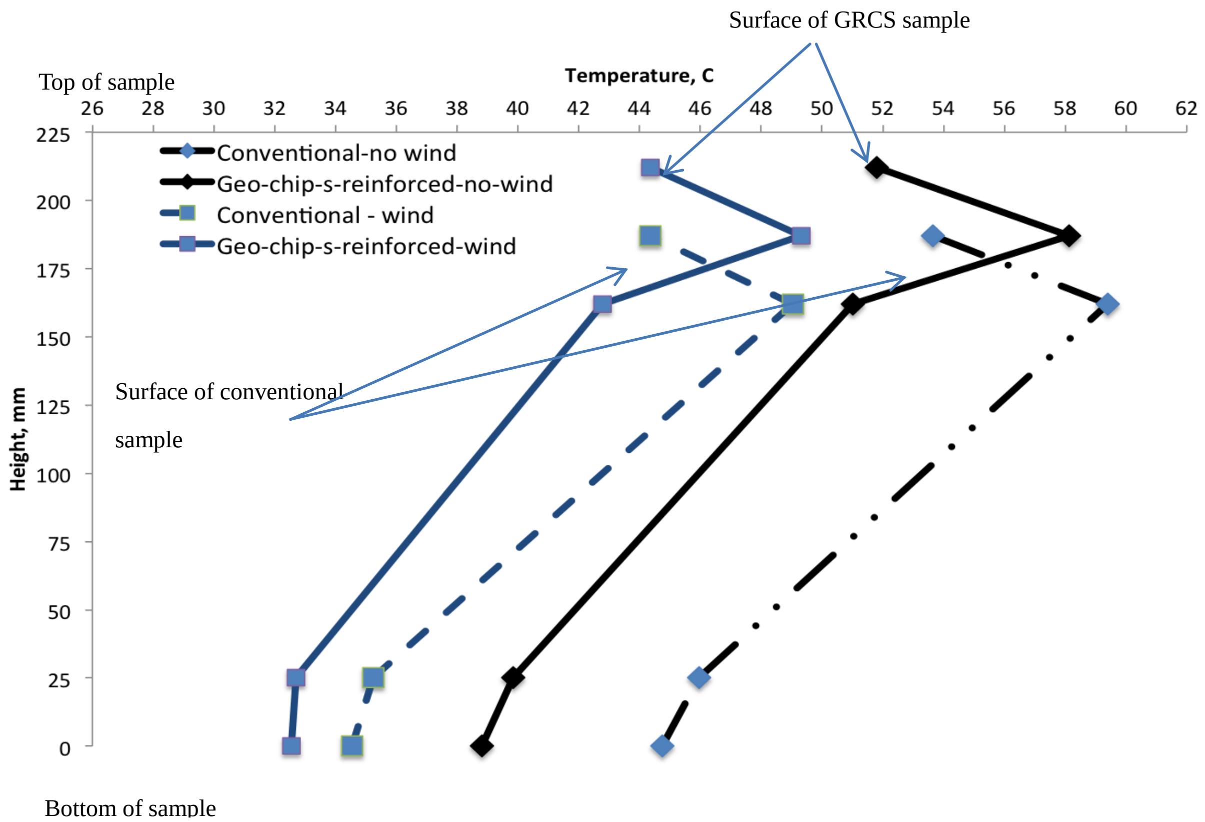

Fig. 9. Plot of Depth versus Temperature (Data Points Obtained from Thermocouple Locations: Surface, 25 mm below Surface, 25 mm from the Bottom, Bottom).

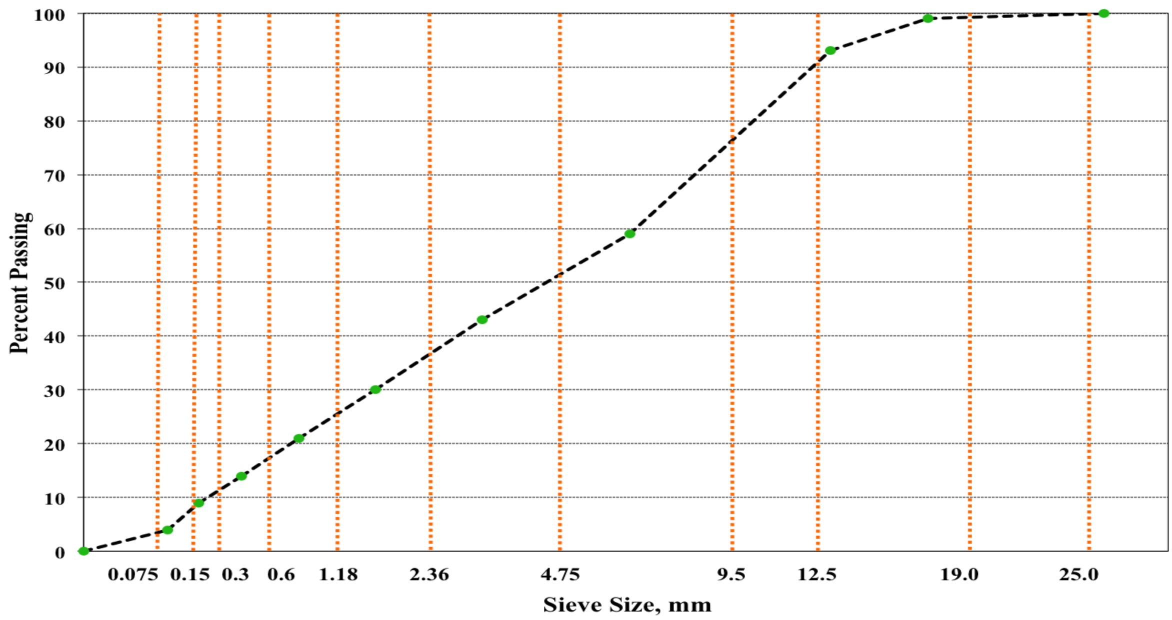

Fig. 10. Gradation of Mix Used in this Study.

sample setup is shown in Fig. 11.

Results of testing from 2 days (marked as day-1 and day-2) are presented – one for relatively cooler day and the other for a relatively warmer day. The ambient temperatures, wind speed and solar radiation for the two days are shown in Table 5. These two days were selected as typical cool and warm days in summer at this location, since the average high temperature at this location in August is 25.2^{o}C. Based on previously obtained data from similar experiments [12] these two days were deemed to be sufficient to evaluate the effect of the GRCS on the temperature profile of the HMA samples. Although the paper could definitely be improved by the inclusion of data from tests conducted on more days, the scope

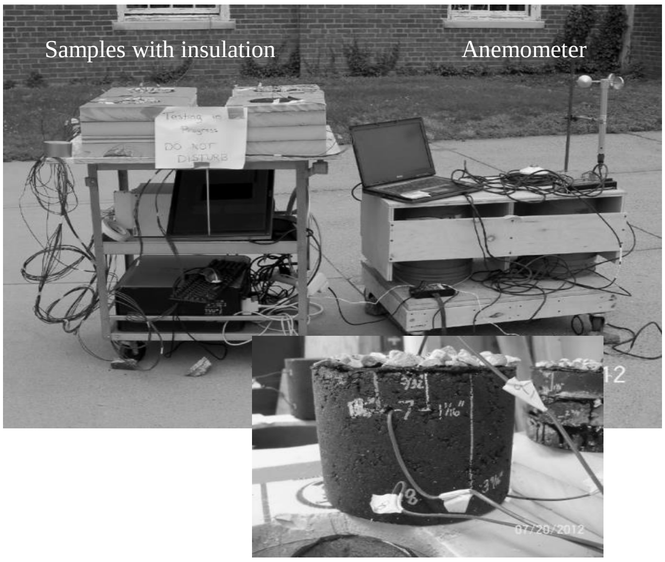

Fig. 11. Test Set-up and Close-up of a Sample with Thermocouples.

Table 5. Environmental Conditions.

Parameter	Day-1	Day-2
Temperature, C	14.25-23.07	19.73-37.84
Solar Radiation, kW/m^2	0.029 - 0.54	0.041-0.887
Wind Speed, Miles Per Hour	0.45 - 5.95	0.11-7.97

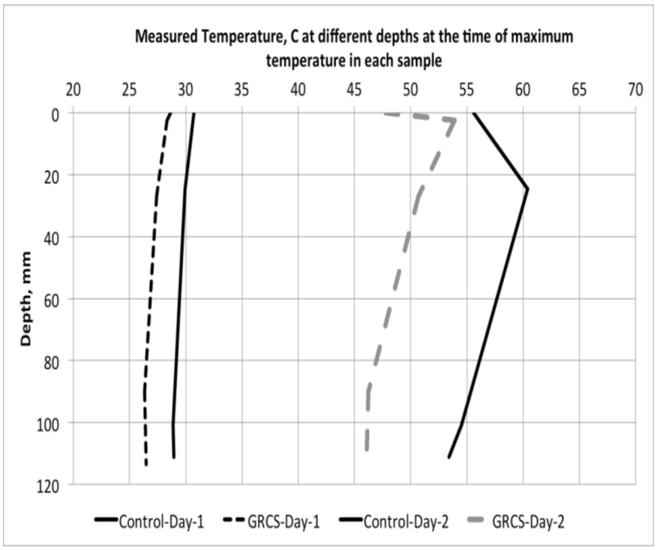

Fig. 12. Temperature at Different Depths at the Time of Maximum Temperature.
Note: control – conventional HMA without any geosynthetic; GRCS – sample with Geosynthetic Reinforced Chip Seal.

of the funding allowed the testing on only two days.

The results of testing are shown in two plots in Fig. 12 and 13. Fig. 12 shows the plots of temperature versus depth at the time when the maximum temperature is reached for each sample whereas Fig. 13 shows the plots of temperature versus time for the different depths.

The data presented in Fig. 12 and 13 show the beneficial effect of the insulation material – it effectively reduces the temperature throughout the depth of the pavement, by up to 10^{o}C, at higher

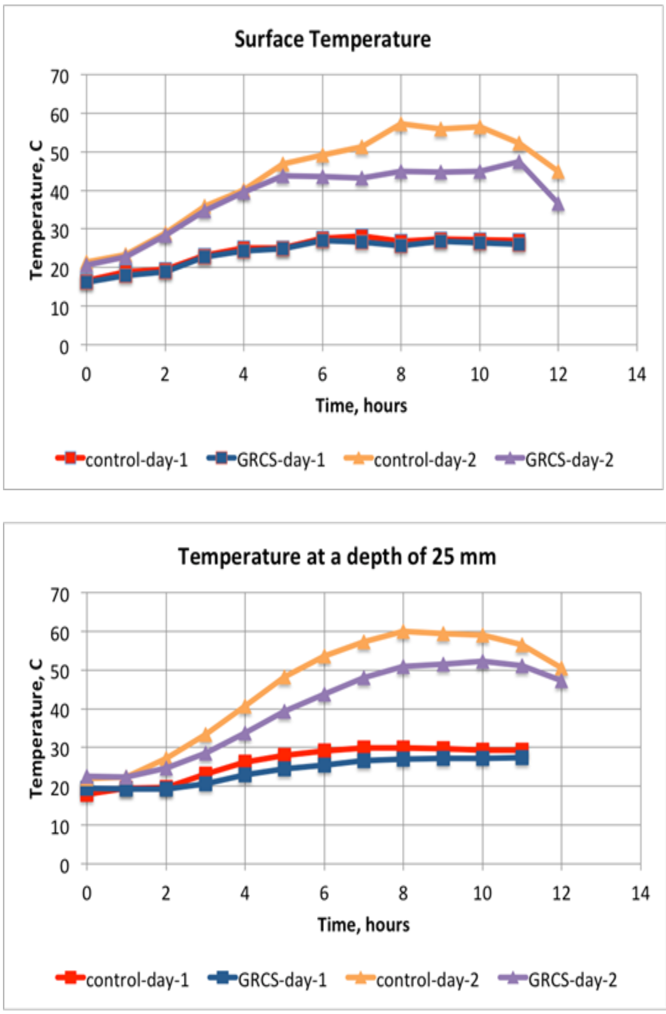

Fig. 13. Temperature Versus Time Plot (Experimental Data); Note: Surface of GRCS Consists of Stones of Chip Seal.

temperatures (day-2), especially near the surface (25 mm below it), and hence reduces the potential of rutting and slows down the aging of the mix.

However, the contribution of the light color aggregates in the chip seal should also be noted, as shown in Fig. 14. It can be seen that the addition of the chip seal (GRCS) reduces the temperature by another 2^{o}C, as compared to the sample with single layer only. It can also be noted that the presence of the asphalt binder in the chip seal coating did not make a difference in the maximum temperature.

If three insulation layers are used instead of one (as seen in Fig. 15), a high reduction in temperature can be obtained, even without the chip seal. This indicates that an increase in thickness of the insulation layer can lead to an increase in the insulation. Note that the two figures, 14 and 15, are from data collected on two separate days to confirm the data. The radiation, wind speed and ambient temperature range for each day are indicated on the respective figures.

Conclusions

From this study it can be concluded that the use of a thermal insulation material is effective in insulating an asphalt pavement

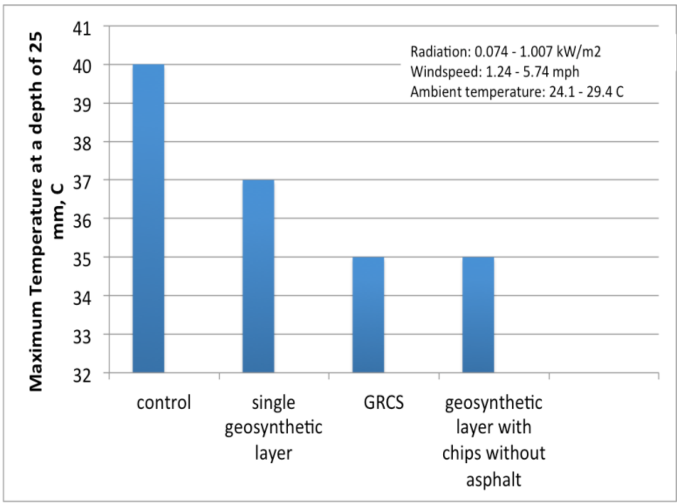

Fig. 14. Comparison of Maximum Temperature at a Depth of 25 mm (Control, Single Geosynthetic Layer, GRCS and Geosynthetic Layer with Chips Only).

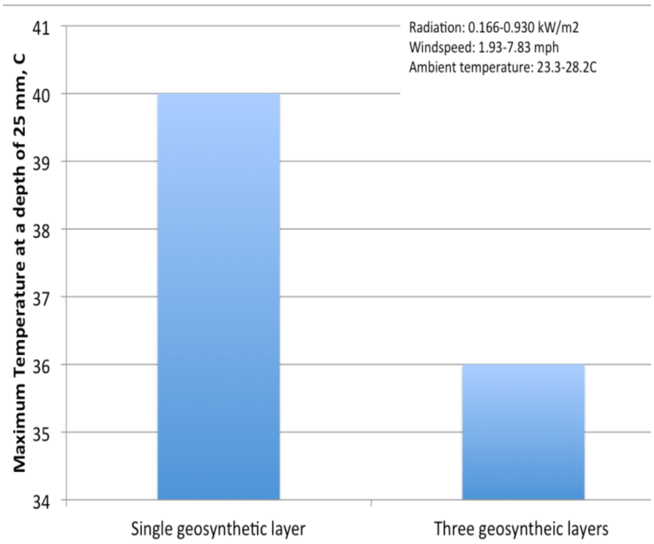

Fig. 15. Comparison of Maximum Temperature at 25 mm Depth between Samples with Single and Three Geosynthetic Layers; Single Layer Thickness = 2mm, Triple Layer Thickness = 6 mm.

from extremes of high temperature. Therefore, it can be postulated that such an application would also reduce the potential of rutting (and aging). The following specific conclusions can be made.

1. The use of GRCS can reduce the temperature in HMA to a significant depth, exceeding 100 mm.
2. The reduction in temperature (compared to conventional HMA) is significant, and ranges from 5 to 12°C, depending on the depth.
3. The use of a greater number of geosynthetic layers can result in a greater reduction of temperature; the use of three layers (instead of one) increased the reduction by 4°C.
4. The use of the high reflectivity chip seal aggregates along with the geosynthetic layer is more beneficial than using the geosynthetic layer alone; the reduction in the case of chip seal with geosynthetic was 2°C more than that in the case of geosynthetic layer only.

Further research is needed to optimize geosynthetic reinforcement systems, with respect to position, thickness (number of layers) and type, for different types of pavements, and investigate the structural impact of GRCS on the pavement performance. The authors specifically recommend the evaluation of the use of this concept for areas that are subjected to high/slow loading at high temperatures, such as intersections in hot climatic locations.

Acknowledgements

This material is based upon work supported by the National Science Foundation under Grant No. 0928397. Any opinions, findings, and conclusions or recommendations expressed in this material are those of the authors and do not necessarily reflect the views of the National Science Foundation. The authors gratefully acknowledge the help of Steve Thaxton of Propex for supplying the materials, and Ryan Worseman and Michael Delph for helping in the preparation of equipment and experiments.

References

1. van de Loo, P.J. (1978). The creep test, a key tool in asphalt mix design and in the prediction of pavement rutting. *Journal of the Association of Asphalt Paving Technologists*, Vol. 47, pp. 253–281.
2. Brown, E.R. and Cross, S.A. (1992). A National Study of Rutting in Hot Mix Asphalt (HMA) Pavements. *NCAT Report 92-5*, National Center for Asphalt Technology, Auburn, Alabama, USA.
3. Wahhab, H.I.A. and Balghunaim, F.A. (1994). Asphalt pavement temperature-related to arid Saudi environment. *Journal of Materials in Civil Engineering*, 6(1), pp. 1–14.
4. Bonaquist, R.J. and Mogawer, W.S. (1997). Analysis of Pavement Rutting Data from FHWA Pavement Testing Facility Superpave Validation Study, *Transportation Research Record*, No. 1590, pp. 80-88.
5. Lu, Y. and Wright, P.J. (2000). Temperature Related Visco-Elastoplastic Properties of Asphalt Mixtures. *Journal of Transportation Eng*ineering, 126(1), pp.58-65.
6. White, T.D., Haddock, J.E., Hand, A.J.T., and Fan, H. (2002). Contributions of Pavement Structural Layers to Rutting in Hot Mix Asphalt Pavements. *NCHRP Report 468*, p. 134, Transportation Research Board, NRC, Washington, DC, USA.
7. Monismith, C.L., Hicks, R.G., Finn, F.M., Sousa, J., Harvey, J., Weissman, S., Deacon, J., Coplantz, J., and Paulsen, G. (1994). Permanent Deformation Response of Asphalt Aggregate Mixes. *SHRP-A-415*, p. 460, Strategic Highway Research Program, Transportation Research Board, NRC, Washington, DC, USA.
8. Traxler, R.N. (1961). Relation between Asphalt Composition and Hardening by Volatilization and Oxidation. *Journal of the Association of Asphalt Paving Technologists*, Vol. 30, pp. 359-377.
9. Traxler, R.N. (1963). Durability of Asphalt Cements. *Journal of the Association of Asphalt Paving Technologists*, Vol. 32, pp. 44-58.

10. Bell, C. (1989) Summary Report on Aging of Asphalt-Aggregate Systems SR-OSU-A-003A-89-2. *SHRP A-305 Report*, p. 121, Strategic Highway Research Program, Transportation Research Board, NRC, Washington, DC, USA.
11. Glanzman, T. (2005). Quantifying the Benefits of Polymer Modified Asphalt, *Asphalt*, pp.18-20, Asphalt Institute, Lexington, Kentucky, USA.
12. Mallick, R.B., Chen, B.L., and Bhowmick, S. (2009). Harvesting Energy from Asphalt Pavements and Reducing the Heat Island Effect. *International Journal of Sustainable Engineering*, 2(3), pp. 214-228.
13. Kawakami, A. and Kubo, K. (2008). Development of a Cool Pavement for Mitigating the Urban Heat Island Effect in Japan. *Proceedings of the 1st International Symposium on Asphalt Pavements and Environment*, International Society for Asphalt Pavements, Zurich, Switzerland, pp. 423-434.
14. Bhowmick, S., Medas, M., and Mallick, R.B. (2012). Role of conductive spreader layer in reducing surface temperature of HMA pavements. *International Journal of Sustainable Engineering*, 5(4), pp. 338-349.
15. Li, H., Harvey, J., and Kendall, A. (2013). Field measurement of albedo for different land cover materials and effects on thermal performance. *Building and Environment,* Vol. 59, pp. 536-546.
16. Bejan, A. (1993). *Heat Transfer*, p. 704, John Wiley & Sons, Hoboken, New Jersey, USA.
17. Solaimanian, M. and, Kennedy, T.W. (1993). Predicting Maximum Pavement Surface Temperature Using Maximum Air Temperature and Hourly Solar Radiation. *Transportation Research Record*, No. 1417, pp.1-11.
18. Chen, B.L., Rockett, L., and Mallick, R.B. (2008). Laboratory Investigation of Temperature Profiles and Thermal Properties of Asphalt Pavements with Different Subsurface Layers. *Journal of Association of Asphalt Paving Technologists*, Vol. 77, pp. 327-360.
19. National Cooperative Highway Research Program (NCHRP) (2004). *Guide for Mechanistic-Empirical Design*. Transportation Research Board, Washington, DC, USA. Online http://onlinepubs.trb.org/onlinepubs/archive/mepdg/guide.htm, Last Accessed December, 2012.
20. COMSOL Multiphisics, version 4.3 (software) (2012). http://www.comsol.com.
21. The Engineering Toolbox, Thermal Conductivity of some common Materials and Gases. Online http://www.engineeringtoolbox.com/thermal-conductivity-d_429.html, Last Accessed December, 2012.
22. Iwama, M, Yshinaka, T, and Nemoto, N. (2006). Development of Surface Treatment Technology Targeting Temperature Reduction of Asphalt Pavement. *Proceedings of the 12th Road Engineering Association of Asia and Australia Conference*, Manila, Philippines, p15.
23. Wan, W and Ping, T. (2009). A Study on the Effectiveness of Heat Mitigating Pavement Coatings in Singapore. *Proceedings of the 2nd International Conference on Countermeasures to Urban Heat Islands*, Berkley, California, USA, p. 12.
24. Synnefa, A, Karlessi, T, Gaitani, N, and Santamouris, M. (2009). Measurement of Optical Properties and Thermal Performance of Coloured Thin Layer Asphalt Samples and Evaluation of Their Impact on the Urban Environment. *Proceedings of the 2nd International Conference on Countermeasures to Urban Heat Islands*. Berkley, California, USA, p. 12.
25. NREL (2012). *National Solar Radiation Database*. http://rredc.nrel.gov/solar/old_data/nsrdb/; accessed October 2012.
26. FHWA (2009). *Pavements: LTPPBind*, Federal Highway Administration, Washington, DC, USA.
27. Sailor, D.J and Dietsch, N. (2005). *The Urban Heat Island Mitigation Impact Screening Tool (MIST)*. Online http://www.heatislandmitigationtool.com/Documents/detailed_help.pdf, Last Accessed November, 2012.
28. California Pavement Preservation Center (2012). Geosynthetic Reinforced Chip Seals. *Newsletter of the California Pavement Preservation Center***.** No. 21, pp. 7-8.